Int. J. Electrochem. Sci., 6 **(2011)** 3743 - 3753

International Journal of
ELECTROCHEMICAL
SCIENCE
www.electrochemsci.org

Immobilization of Cytochrome c on Multi-Walled Carbon Nanotube-Poly(Vinysulfonic Acid) Composite Film and Its Application for Amperometric Determination of H_2O_2

Yan-Ling Yang, Binesh Unnikrishnan, Shen-Ming Chen[*]

Electroanalysis and Bioelectrochemistry Lab, Department of Chemical Engineering and Biotechnology, National Taipei University of Technology, No. 1, Section 3, Chung-Hsiao East Road, Taipei 106, Taiwan, ROC
[*]E-mail: smchen78@ms15.hinet.net

Received: 17 July 2011 / *Accepted:* 19 August 2011 / *Published:* 1 September 2011

We report the immobilization of Cytochrome c (Cyt c) on multi-walled carbon notube-poly(vinyl sulfonic acid) (MWCNT-PVS) composite film modified glassy carbon electrode (GCE) and its application as H_2O_2 sensor. The MWCNT-PVS film is a good matrix for the immobilization of Cyt c. The surface morphological studies by atomic force microscopy (AFM) and electrochemical impedance spectroscopy (EIS) characterization of the film confirmed the presence of Cyt c in the film. The cyclic voltammetric (CV) responses of Cyt c MWCNT-PVS in pH 7 exhibit prominent redox couple for the $Fe^{III/II}$ redox process with a peak-to-peak separation (ΔE_p) of 55 mV. The composite film showed good electrocatalytic activity towards the reduction of H_2O_2 in pH 7. Amperometric i-t responses of MWCNT-PVS/Cyt c composite modified rotating disc glassy carbon electrode towards the H_2O_2 reduction were recorded at the applied potential of – 0.2 V. The rotation speed was 1200 RPM. The modified electrode showed a wide linear range of detection from 10 x 10^{-6} to 7.5 x 10^{-4} M H_2O_2. The stable background current, quick response and wide linear range demonstrate the possibilities of the proposed film for its potential application in real sample analysis.

Keywords: Multi-walled carbon nanotubes, Cytochrome c, direct electrochemistry, amperometry, H_2O_2, composite film, modified electrodes, electrochemical impedance spectroscopy**.**

1. INTRODUCTION

Hydrogen peroxide (H_2O_2) is an important compound in organic synthesis, pharmaceutical and chemical industries due to its excellent oxidant properties. H_2O_2 is also used in many cleaning and antiseptic solutions. Thus, these industries are sources of H_2O_2 to the environment. Thunder and lighting also produce H_2O_2 and cause acid rain [1] and are sources of H_2O_2 in natural waters. Rain

water samples tested before and after thunder and lightning showed about five times increase in H_2O_2 concentration [2, 3]. H_2O_2 is toxic in nature and can cause detrimental effects on biological systems and contribute to the neuropathology of central nervous system [4]. H_2O_2 can cause damages to several regions of brain [5]. So, it is a major concern to clinic, environment, food and chemical industries [6]. Therefore, the determination of H_2O_2 in water, food and clinical samples [7], industrial processing and environmental protection [8] is very important. Several methods have been developed for its determination in trace amounts. However, electrochemical measurements are preferred over the conventional methods [9-11] due to low cost, fast response and easy handling. Enzyme based biosensors are operated at a small potential window in the region of their redox couple. This gives them the advantage of high selectivity avoiding interferences to a great extent [12-13]. Heme group containing proteins and enzymes are widely used for electrochemical reduction and determination of H_2O_2.

Cytochrome c (Cyt c) is a redox protein with a heme group which has an $Fe^{III/II}$ redox center. It is an electrochemically well characterized redox protein [14]. Plenty of reports are available for the direct electrochemistry of Cyt c [15-19]. However, direct electrochemistry of Cyt c is very difficult to obtain due to some conformational changes occurring during its adsorption on metal electrode surface [20]. During the conformational changes, the heme group takes an unfavorable orientation with respect to the electrode, making the electron transfer process difficult. Therefore, choosing a suitable matrix is very important for immobilization of Cyt c. The interface must have good electron transfer kinetics, and that is possible through electrode modification [14]. Carbon nanotubes are a good choice of matrix [21] for electrode modification due to their high mechanical strength, electrical, thermal and electrocatalytic properties. The pristine MWCNT is hydrophobic in nature which is not soluble in polar solvents and not suitable for immobilization of biomolecules. Therefore, MWCNT are either functionalized and or used as composites with surfactants, conducting polymers, polyelectrolytes etc. In this work, we functionalized the MWCNT by sonochemical treatment to increase the hydrophilic nature and to generate more negatively charged sites on the surface. Then, the functionalized MWCNT was dispersed in poly(vinylsulfonic acid) (PVS) which increases the negatively charged sites on the multi-walled surface and helps to make strong electrostatic interactions with positively charged Cyt c. It was applied for the electrochemical determination of H_2O_2.

2. MATERIALS AND METHODS

2.1. Apparatus

A CHI 611A electrochemical workstation was used to carryout out all cyclic voltammetric experiments. A conventional three electrode system with MWCNT, PVS, MWCNT-PVS and MWCNT-PVS/Cyt c modified GCE as working electrodes, a thin Pt wire as counter electrode and Ag/AgCl (sat. KCl) as reference electrode was used for all electrochemical measurements. Electrochemical impedance spectroscopy (EIS) measurements were done using IM6ex ZAHNER (Kroanch, Germany). Scanning electron microscopy (SEM) was performed using a Hitachi S-3000 H

Scanning Electron Microscope. A CHI 750 potentiostat with analytical rotator AFMSRX (PINE Instruments, USA) was used for amperometric experiments.

2.2. Reagents and materials

Bovine heart Cytochrome c (95% purity) was obtained from Sigma-Aldrich. Poly(vinylsulfonic acid sodium salt) 25% solution in water was obtained from Aldrich, USA. MWCNT with O.D. 10 – 15 nm, I.D. 2–6 nm and length 0.1–10 μm obtained from Sigma–Aldrich was used after pretreatment with acid. 0.1 M phosphate buffer solution (PBS) was prepared from 0.1 M Na_2PO_4 and NaH_2PO_4 in doubly distilled deionized water to get a pH of 7. 1mg/mL Cyt c solution was prepared in 0.1M PBS (pH 7). Inert atmosphere was set by passing purified N_2 gas over the solution during experiment. All the experiments were conducted at ambient temperature (25ºC ± 2ºC).

2.3. Fabrication of MWCNT-PVS/Cyt c modified GCE

MWCNT was pretreated following the procedures reported elsewhere [22, 23]. 150 mg of MWCNT was heated at 350ºC for 2 h and allowed to cool down to room temperature to remove any volatile impurities. Then it was ultrasonicated for 4 h in concentrated HCl to remove impurities like amorphous carbon and metal catalysts. It was filtered and washed thoroughly with deionized water until the pH of the washing was 7. The filtered MWCNT was dried at 100ºC for 1 h. The purified MWCNT was treated by ultrasonication in a mixture of sulfuric acid and nitric acid in 3:1 ratio for 6 h. It was then washed several times with deionized water, until the washing was neutral and dried. 1 mg of the pretreated MWCNT was dispersed into 1 mL of 1% PVS solution by ultrasonication for 30 min. A well dispersed homogeneous solution of 1 mg mL^{-1} MWCNT in PVS was obtained. To fabricate the MWCNT-PVS modified electrodes, the GCE was polished using 0.05 μm alumina slurry and Buehler polishing cloth. The GCE was washed and then ultrasonicated in deionized water and ethanol for 5 min each to remove any adsorbed alumina particles on the electrode surface. 3 μL of MWCNT-PVS dispersion was drop casted onto the well polished GCE surface and dried at 50ºC. Then 3μL of Cyt c solution was drop coated and dried at room temperature.

3. RESULTS AND DISCUSSIONS

3.1 Surface morphological characterization by AFM

Fig. 1 shows the AFM images of Cyt c and MWCNT-PVS/Cyt c composite films coated on indium tin oxide (ITO) electrode with identical conditions mentioned for the GCE modification in section 2.3. Fig. 1 (a) shows the AFM image of Cyt c and (b) shows the MWCNT-PVS/Cyt c composite film. Both the images have difference surface morphologies. From fig.1 (b) it is clear that MWCNTs, PVS and Cyt c form a composite with MWCNT visible at some places. Fig 1 (c) is the magnified view of the MWCNT-PVS/Cyt c composite film, which show the presence of MWCNT,

PVS and Cyt c as a three dimensional matrix with compact structure. Sonochemical treatment of MWCNT in acid produces oxygen containing functionalities on the MWCNT surface [24]. The functional groups possess negative charges in pH 7.

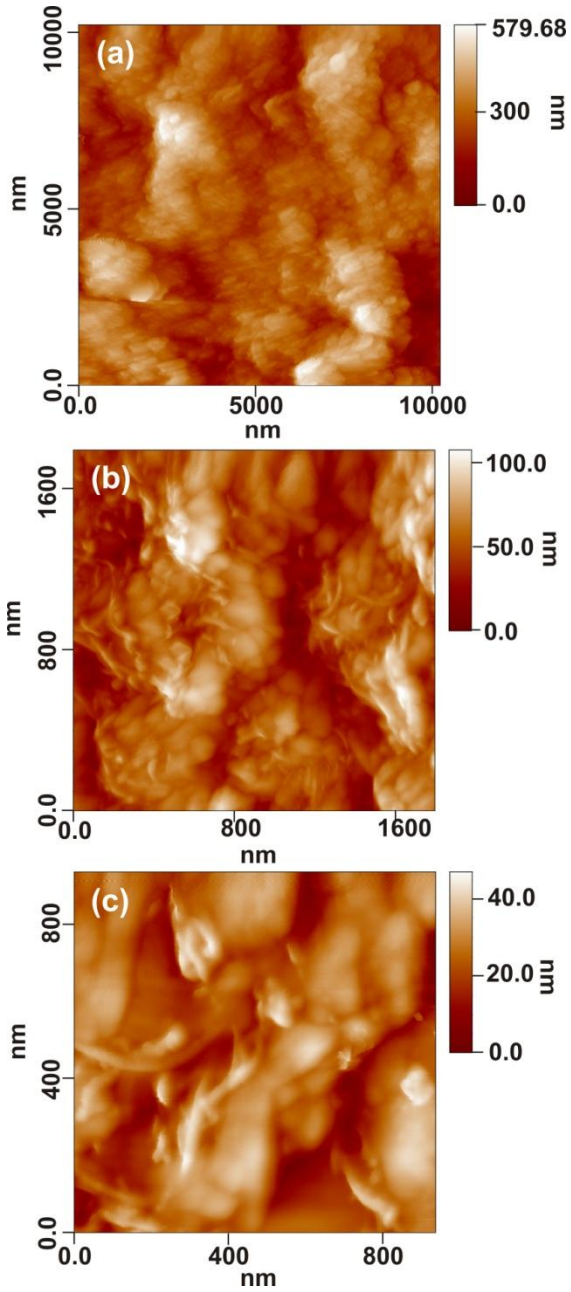

Figure 1. AFM images of (a) Cyt c, (b) MWCNT-PVS/Cyt-c and (c) magnified image of (b)

Moreover, the $-SO_3^-$ groups present in PVS add more negatively charged sites in the MWCNT-PVS film. Cyt c possesses a net positive charge in pH 7 [25]. We prepared Cyt c solution in pH 7 (0.1M PBS) and also the experiments were conducted in pH 7. Therefore, the positively charged Cyt c interacts electrostatically with the negatively charged MWCNT-PVS matrix and forms a stable composite.

3.2 Electrochemical Impedance spectroscopy studies

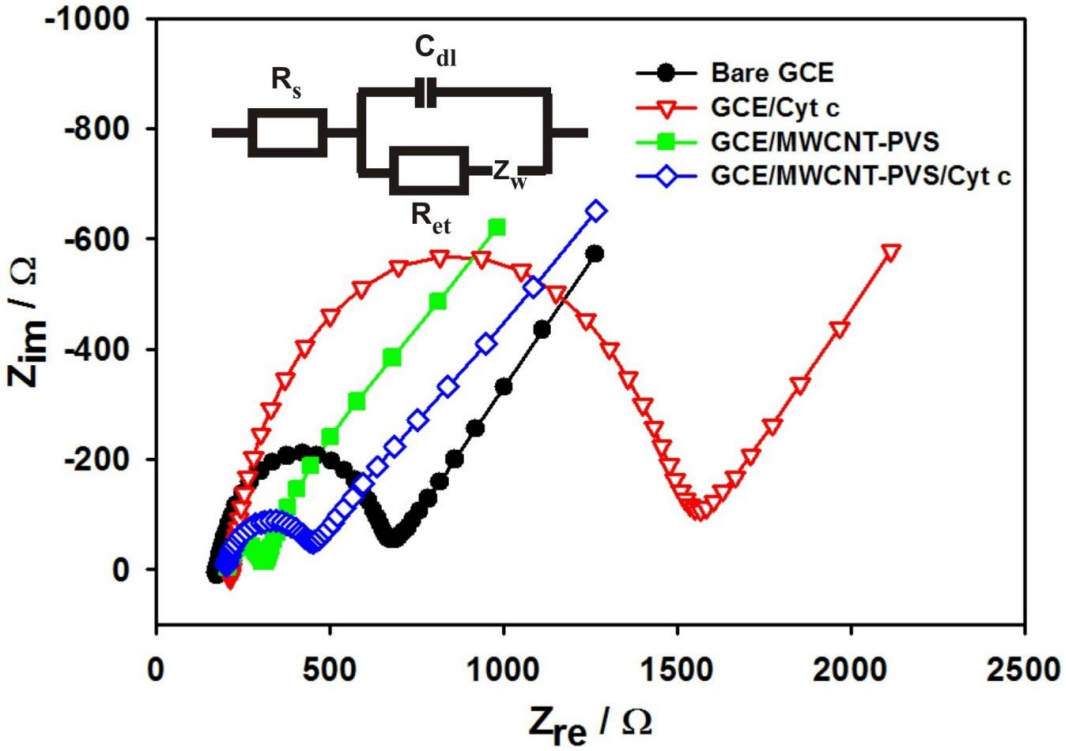

Figure 2. Nyquist plot for bare GCE, GCE/Cyt c, GCE/MWCNT-PVS, and GCE/MWCNT-PVS/Cyt c obtained from EIS measurements in 5 mM $Fe(CN)_6^{3-}/Fe(CN)_6^{4-}$ in PBS. Applied AC voltage: 5mV, frequency: 0.1 Hz to 100 kHz.

Enzymes, proteins, conducting polymers or semiconducting materials change the double layer capacitance and interfacial electron transfer resistance of electrodes after electrode modification. EIS can reveal the impedance changes on the corresponding electrode surface. The inset of fig.2 shows the Randles equivalence circuit model used to fit the experimental data. Where, R_s represents the electrolyte resistance, R_{et} is the charge transfer resistance, C_{dl} double layer capacitance and Z_w is the Warburg impedance. Fig. 2 shows the Nyquist plot of EIS for bare GCE, GCE/Cyt c, GCE/MWCNT-PVS, and GCE/MWCNT-PVS/Cyt c in 5 mM $Fe(CN)_6^{3-}/FE(CN)_6^{4-}$ in PBS. Applied AC voltage: 5 mV, frequency: 0.1 Hz to 100 kHz. The electron transfer resistance (R_{et}) of the electrode is equal to the semi circle appearing in the Nyquist plot. All the films show semi circles of different diameters exhibiting different R_{et}. Compared to the bare GCE, GCE/Cyt c shows a larger semicircle indicating a high charge transfer resistance. This is due to the poor conducting nature of Cyt c. The addition of MWCNT-PVS onto the bare GCE reduces the R_{et} due to the very good conducting nature of MWCNT. The GCE/MWCNT-PVS/Cyt c film shows a higher electron transfer resistance than GCE/MWCNT-PVS which confirms the immobilization of Cyt c on the composite electrode. These results confirm the presence of MWCNT/PVS and Cyt c in GCE/MWCNT-PVS/Cyt c film. The electrostatic interaction of positively charged Cyt c and the negatively charged oxygen containing functionalities and the $–SO_3^-$ of PVS enhance the overall electron transfer performance of the proposed film.

3.3 Electrochemical behavior of MWCNT-PVS/Cyt c modified GCE in 0.1 M PBS

The electrochemical behavior of the modified electrodes have been studied by CV. Fig. 3 shows the cyclic voltammograms recorded in 0.1 M (pH 7) for various electrodes at a scan rate of 0.05 Vs^{-1}. Purified N_2 gas was purged into the buffer solution for 30 min to remove dissolved oxygen before recoding CV. Curve (a) of fig. 1 shows the CV response of GCE/Cyt c. No obvious peaks appear for Cyt c on GCE. Curve (b) is CV response of GCE/MWCNT/Cyt c. Cyt c shows small hump or shoulder peaks for the redox process. The cathodic peak appears at – 0.290 V and the anodic peak appears at – 0.215 V. The (ΔEp) is 75 mV. GCE/MWCNT-PVS (curve b) shows a redox couple, oxidation peak appearing at – 0.002 V and the reduction peak appearing at – 0.056 V. This redox couple is due to the presence of quinone like surface bound oxygen containing functional groups on the MWCNT surface, which are formed during the acid treatment [26].

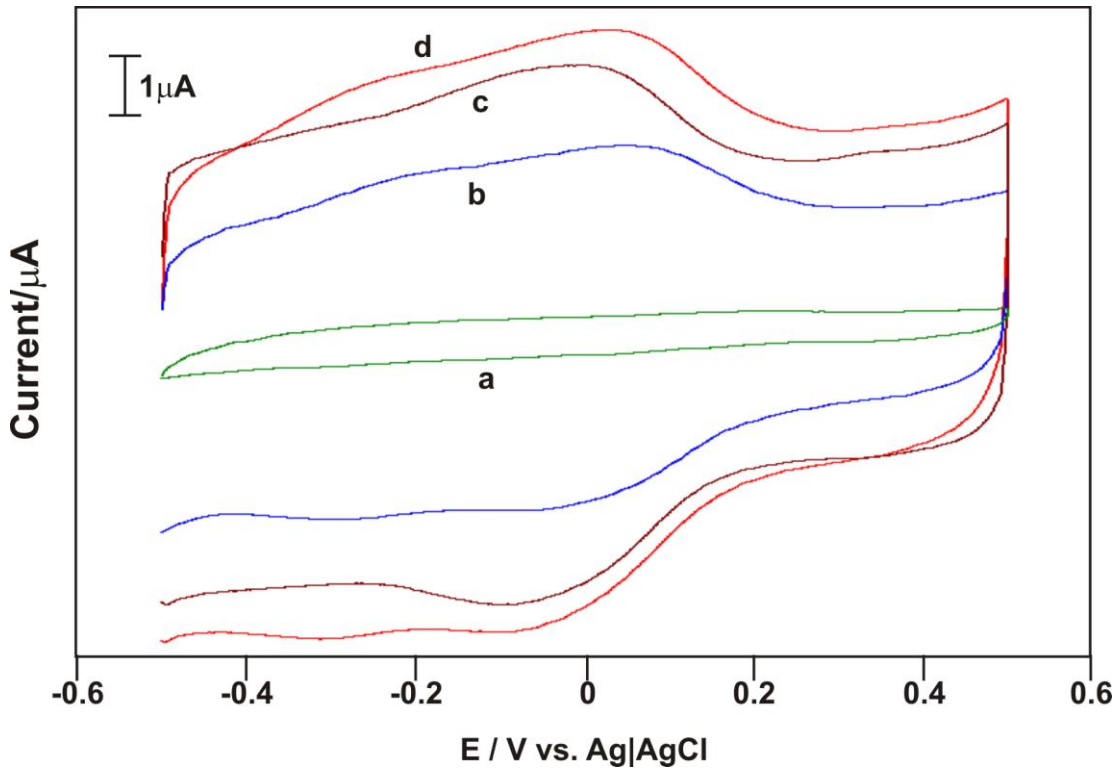

Figure 3. Cyclic voltammograms of different films in 0.1M PBS (pH 7) obtained at a scan rate of 0.05 Vs^{-1} in the potential range of -0.5 to 0.5 V. a) GCE/Cyt c, b) GCE/MWCNT/Cyt c, c) GCE/MWCNT-PVS and d) GCE/MWCNT-PVS/Cyt c

For GCE/MWCNT-PVS/Cyt c, more enhanced redox peaks are observed. The oxidation peak at –0.260 V and reduction peak at – 0.315 V, with peak-to-peak separation (ΔE_p) = 55 mV. This reversible redox couple corresponds to the $Fe^{III/II}$ redox process of Cyt c. This confirms the presence of Cyt c in the film. PVS in the film enhances the MWCNT loading and thus increases the current in both the GCE/MWCNT-PVS and GCE/MWCNT-PVS/Cyt c electrodes. These results show that MWCNT-PVS film provides facile electron transfer between the heme groups of Cyt c and the electrode.

3.3.1 Different scan rate studies

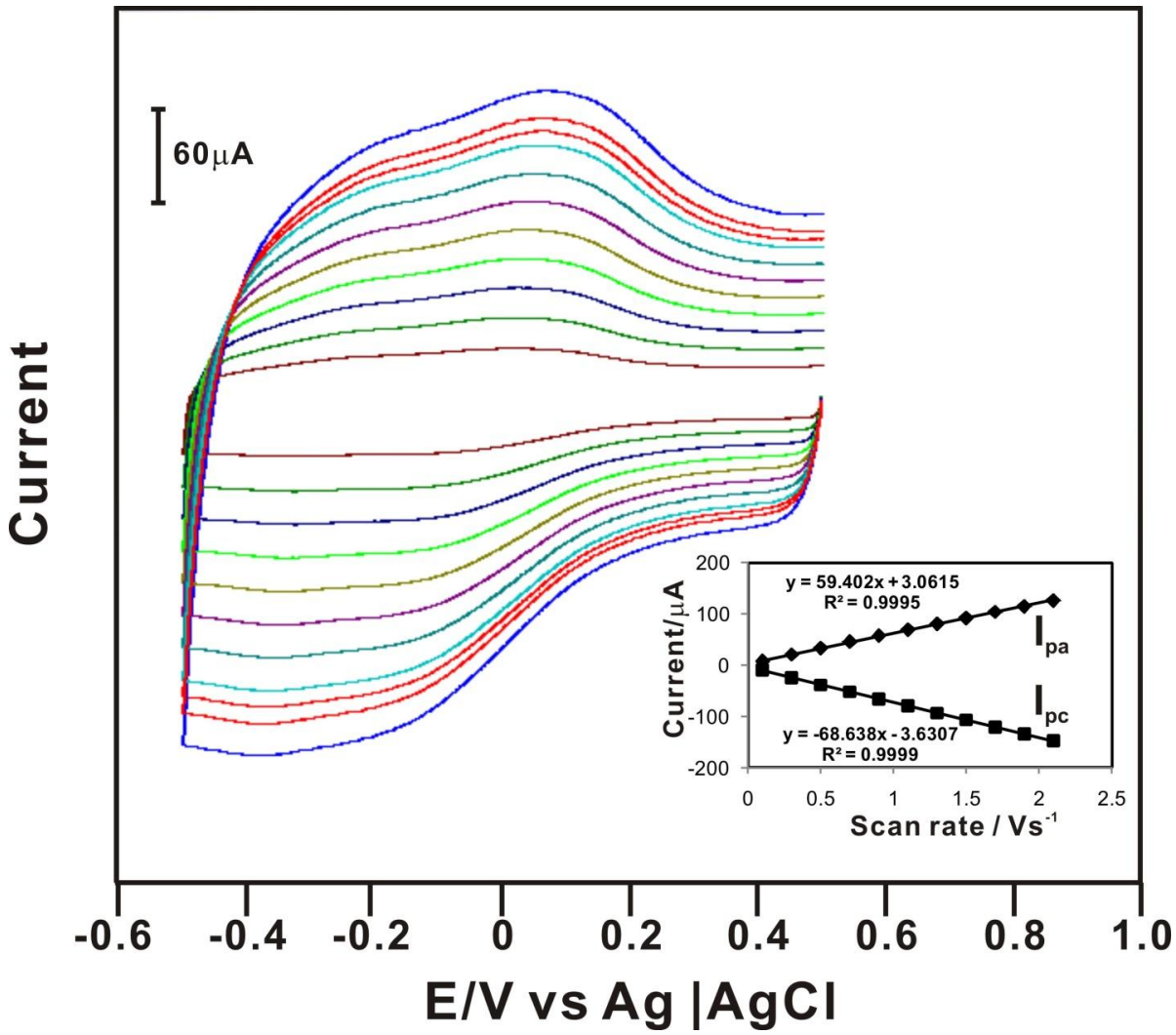

Figure 4. Cyclic voltammograms recorded at GCE/MWCNT-PVS/Cyt c in N_2 saturated 0.1 M PBS (pH 7) with different scan rates. From inner to outer: 10 to 210 mVs^{-1}. Potential range: 0.5 to – 0.5 V. The inset shows the linear dependence of I_{pc} and I_{pa} on scan rates.

The influence of the scan rate on the electrochemical behavior of GCE/MWCT-PVS/Cyt c was investigated using CV in the potential range of - 0.5 to 0.5 V in N_2 saturated 0.1 M PBS (pH 7). Fig. 4 shows the dependence of peak currents on scan rates from 10 to 210 mVs^{-1}. The anodic peak current (I_{pa}) and the cathodic peak current (I_{pc}) of the $Fe^{III/II}$ redox couple of the heme group of Cyt c increase linearly with the increase in scan rate. The linear dependence of I_{pa} and I_{pc} on scan rate is given in the inset of the fig.4. The linear regression equation for the I_{pa} on scan rate is given by I_{pa} (μA) = 59.402 ν + 3.0615 with a correlation coefficient R^2 = 0.9995 and I_{pc} = – 68.638 ν – 3.6307 and correlation coefficient R^2 = 9999. Where, ν is the scan rate in Vs^{-1}. Both cathodic and anodic peak potentials do not change with the different scan rate which indicates the fast electron transfer between Cyt c and the electrode. These results prove that the electrochemical process taking place at GCE/MWCT-PVS/Cyt c electrode surface is a surface confined process and not a diffusion controlled process.

3.3.2 Influence of pH on the electrochemical behavior of GCE/MWCNT-PVS/Cyt c

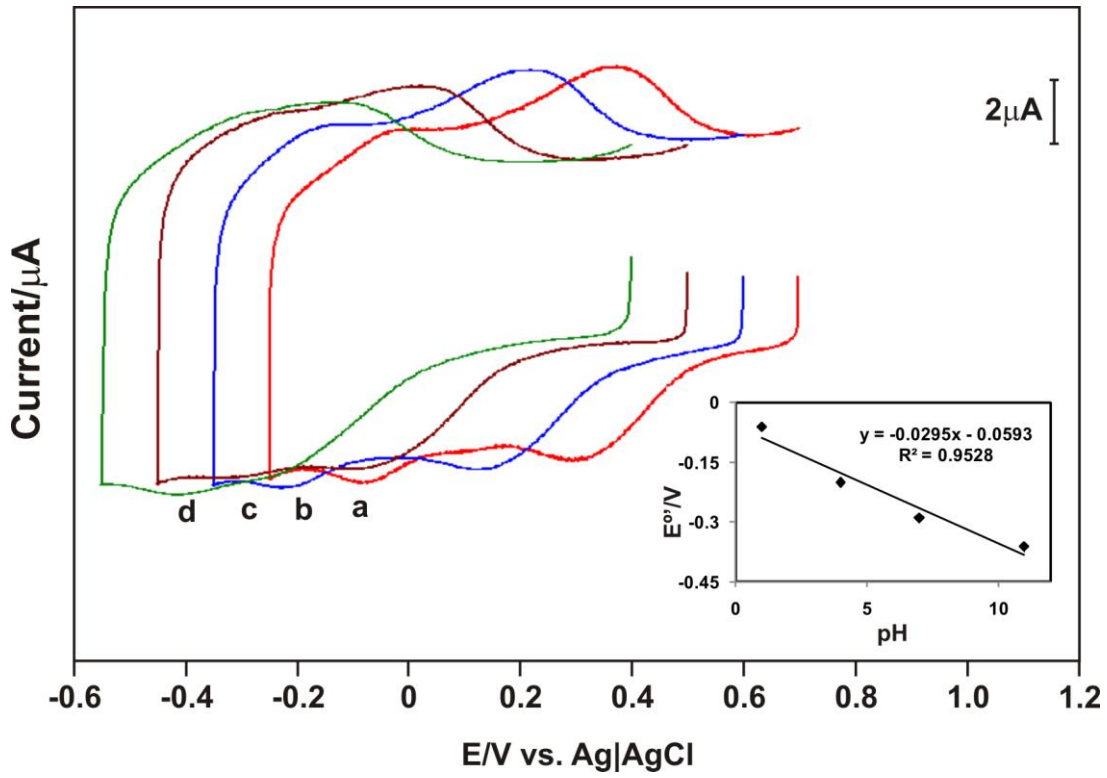

Figure 5. Cyclic voltammograms of MWCNT-PVS/Cyt c modified GCE at 0.05Vs^{-1} against Ag/AgCl reference electrode in different pH solutions (a-d are 1,4,7 and 11) saturated with N_2. The Inset shows the influence of pH on the formal potential with a slope of – 29.5 mV/pH.

In order to study the influence of pH on the electrochemical properties of GCE/MWCNT-PVS/Cyt c, CVs were recorded in various pH aqueous buffer solutions with a scan rate of 0.05 Vs^{-1} against Ag/AgCl as reference electrode. The results are shown in fig.5. CVs were recorded in the pH range 1 to 11. The GCE was modified as mentioned in section 2.3, washed with deionized water to remove any loosely adsorbed Cyt c and then transferred to various pH solutions to record CV. The results show that the formal potential ($E^{o'}$) of $Fe^{III/II}$ redox couple of Cyt c shifts negatively with increase in pH. The negative shift of the formal potential with the change in pH is given in the inset of fig. 5. We obtained a slope value of 29.5 mV/pH, which is close to the theoretical value for a proton process [27-29]. We chose the physiological pH 7 to carry out all the experiments in this project.

3.4. Electrocatalytic reduction of H_2O_2 at GCE/MWCNT-PVS/Cyt c

Fig. 6 shows the electrocatalytic activity of GCE/MWCNT-PVS/Cyt c towards H_2O_2 reduction in 0.1M PBS (pH 7). The reduction peak appears at -0.20V Vs Ag/AgCl. I_{pc} increases linearly with the addition of H_2O_2 (curve b-m in fig.6). At the same time the I_{pa} decreases with the increase in

concentration of H_2O_2 which reveals the good electrocatalytic activity of GCE/MWCNT-PVS/Cyt c towards the reduction of hydrogen peroxide.

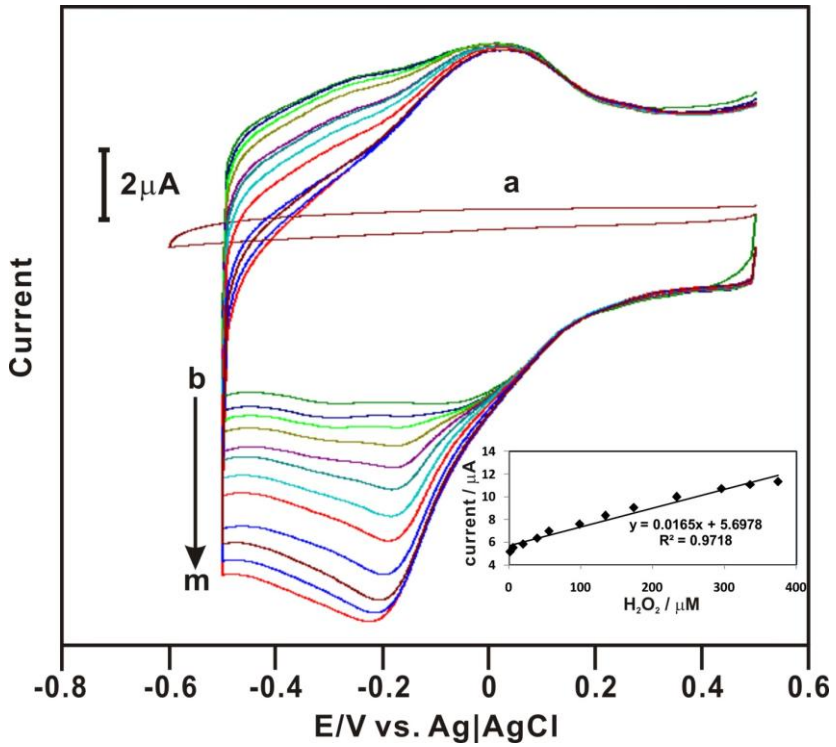

Figure 6. Cyclic voltammograms recorded for various concentrations of H_2O_2 at MWCNT-PVS/Cyt c modified GCE in 0.1 M PBS (pH 7) at a scan rate of 0.05 Vs^{-1}. Potential range: 0.5 to -0.5 V vs Ag/AgCl. a) bare GCE in 375 μM H_2O_2, b) 2, c) 6, d) 20, e) 40, f) 56, g) 99, h) 135, i) 174, j) 234, k) 296, l) 336 and m) 375 μM H_2O_2. The inset shows the linear dependence of the reduction peak current with the concentration of H_2O_2.

However, the anodic peak of the redox couple of functional groups on MWCNT does not show any change with the addition of H_2O_2 indicating that it is not catalyzing the reduction of H_2O_2. Therefore the reduction peak at –0.2 V is due to the electrocatalytic activity of of Cyt c immobilized on the MWCNT-PVS matrix. I_{pc} increases with the increase in H_2O_2 concentration from 2 to 375 μM. The inset of fig. 6 shows the linear dependence of I_{pc} with H_2O_2 concentration. The linear regression equation for the reduction is I_{pc} (μA) = 0.0165 μM + 5.6978 with correlation coefficient R^2 = 0.9718. This shows the excellent electrocatalytic activity of the proposed film towards H_2O_2 reduction and its promising application as an H_2O_2 sensor. Hence, -0.2V vs Ag/AgCl is set for the amperometric determination of H_2O_2 in our experiment.

3.5 Amperometric response of MWCN-PVS/Cyt c modified GCE towards H_2O_2 reduction

Rotating disc electrode is a hydrodynamic electrochemical technique which involves the convective mass transport of reactants and products at the electrode surface, when the electrode is rotated at a specific speed [30]. The amperometric experiments where conducted with rotating disc

GCE with a surface area of 0.236 cm^2. The surface modification and Cyt c immobilization were done as mentioned in section 2.3. Fig. 7 shows the amperometric response of MWCNT-PVS/Cyt c composite film modified rotating dick GCE in N_2 saturated PBS. The applied electrode potential was – 0.2 V and the rotation speed was 1200 RPM. The film shows quick response to the addition of H_2O_2.

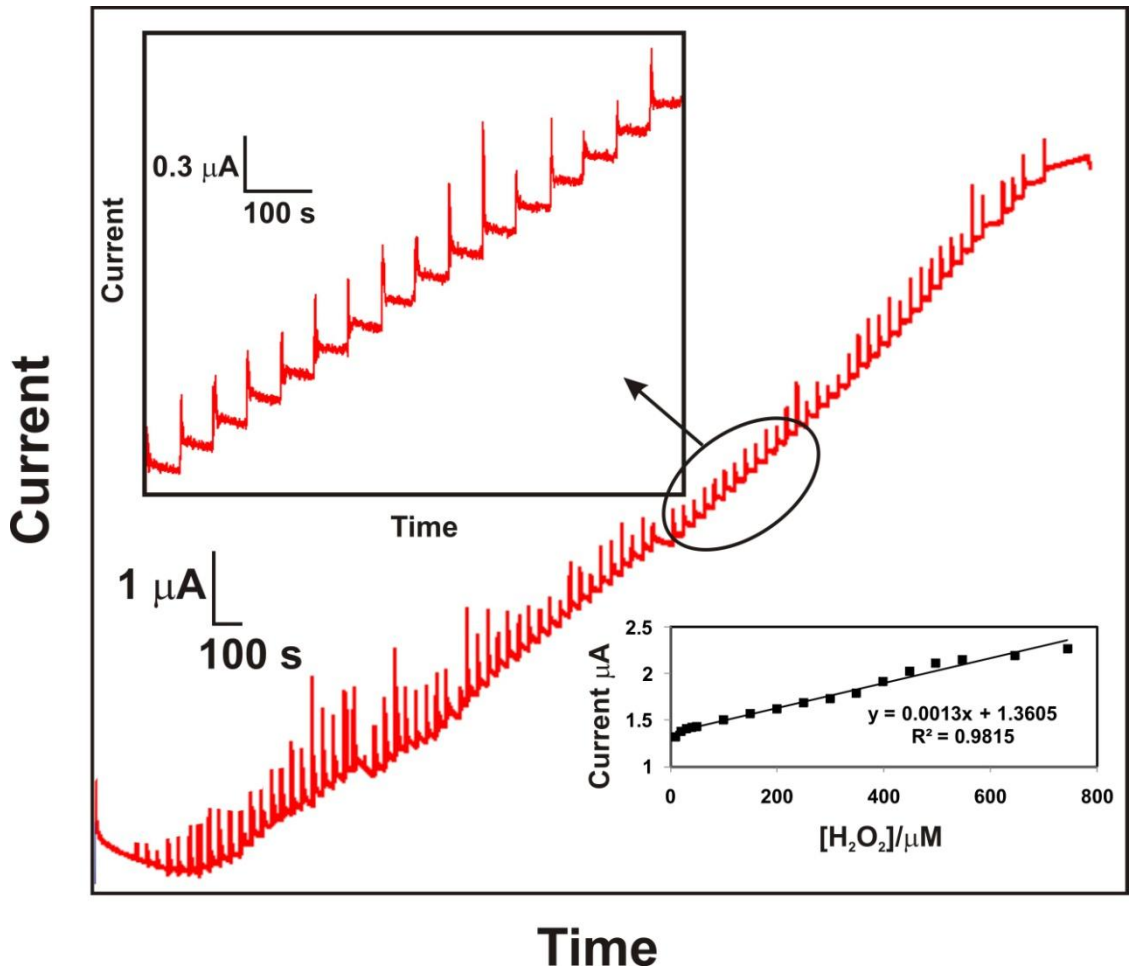

Figure 7. Amperometric i–t curve of MWCNT-PVS/Cyt c modified rotating disc GCE at an applied potential of − 0.2 V for the addition of 2 x 10^{-6} to 3.428 x 10^{-3} M H_2O_2 in N_2 saturated 0.1 M PBS (pH 7) . Rotation rate: 1200 RPM. The inset shows the plot of linear dependence of peak current on H_2O_2 concentration.

The sensor shows a linear increase in current when the concentration of the H_2O_2 in the solution from 10 x 10^{-6} M. The inset of fig. 7 shows the linear dependence of the current with H_2O_2 concentration. The linearity regression equation for the response is I (μA) = 0.0013 μM + 1.3605. The correlation coefficient R^2 = 0.9815. From the current vs concentration curve, the linear range of the film for H_2O_2 detection was determined as 10 x 10^{-6} to 7.5 x 10^{-4} M H_2O_2. The film exhibits a sensitivity of 0.0055 μA μM^{-1} cm^{-2}. The proposed film may be optimized for real life applications as H_2O_2 biosensor.

4. CONCLUSIONS

We demonstrated a simple procedure to fabricate MWCNT-PVS/Cyt c composite for H_2O_2 sensing application. The film showed good stability and good catalytic activity towards the reduction of H_2O_2. The surface morphological and electrochemical characterization of the film revealed the presence of Cyt c in the film. The stability of the film could be due to the electrostatic interaction of both the negatively charged functionalized MWCNT and poly (vinylsulfonic acid) with the positively charged Cyt c in pH 7. The performance of the propose film is promising in the development of a real life H_2O_2 biosensor.

References

1. Y. Komazaki, T. Inoue and S. Tanaka, *Analyst,* 126 (2001) 587.
2. Y. Deng and Y. Zuo, *Atmos. Environ.*, 33 (1999) 1469.
3. T. Tanaikai, A.Sakuragawa, and T. Okutani, *Anal. Sciences*, 16 (2000) 275.
4. Elizabeth A. Mazzio and Karam F. A. Soliman, *J. Appl. Toxicol.*, 24 (2004) 99.
5. M. B Youdim and L. Lavie, *Life Sci.*, 55 (1994) 2077.
6. A.K. M Kafi, G. S. Wu, and A. C. Chen, *Biosens. Bioelectron.*, 24 (2008) 566.
7. X. B. Lu, J. H. Zhou, W. Lu, Q. Liu and J.H. Li, *Biosens.Bioelectron.*, 23 (2008) 1236.
8. X. H. Shu, Y. Chen, H. Y. Yuan, S. F. Gao and D. Xiao, *Anal. Chem.*, 79 (2007).
9. D. Marchington, H.C.E. McGovan and N.V. Klassen, *Anal. Chem.*, 66, 2921 (1994).
10. A Pralle M.C.Y. Chang, E.Y. Isacoff and C.J. Chang, *J. Am. Chem. Soc.*, 126, 15392 (2004) 3695.
11. C. Matsubara, N. Kawamoto and K. Takamura,, *Analyst*, 117 (1992) 1781.
12. Y. H. Wu and S. S. Hu, *Microchim. Acta*, 159 (2007) 1.
13. L. Gorton, *Electroanal.*, 7 (1995) 23.
14. F. A. Armstrong, H. A. O. Hill and N. J. Walton, *Acc. Chem. Res*, 21 (1988) 407.
15. T. Lu, X. Yu, S. Dong, C. Zhon, S. Ye and T.M. Cotton, *J. Electroanal. Chem.*, 369 (1994) 79.
16. C. Cai, *J. Electroanal. Chem.*, 393 (1995) 119.
17. R. M. Iost, J. M. Madurro, A. G. B. Madurro, I. L. Nantes, L. Caseli and F. N. Crespilho, *Int. J. Electrochem. Sci.*, 6 (2011) 2965.
18. A. Balamurugan and S. M. Chen, *Biosens. Bioelectron.*, 24 (2008) 976.
19. S. M. Chen and S. V. Chen, *Electrochim. Acta,* 48 (2003) 513.
20. J. E. Frew and H. A. O. Hill, *Eur. J. Biochem.* , 172 (1988) 261.
21. J. W. Shie, U. Yogeswaran and S. M. Chen, *Talanta*, 74 (2008) 1659.
22. D. R. S. Jeykumari, S. Ramaprabhu and S. S. Narayanan, *Carbon*, 45 (2007) 1340.
23. H. Su, R. Yuan, Y. Chai, Y. Zhuo, C. Hong, Z. Liu, X. Yang, *Electrochim. Acta*, 54 (2009) 4149.
24. Y. Xing, L. Li, C. C. Chusuei, and R.V. Hull, *Langmuir*, 21 (2005) 4185.
25. Y. Goto, N. Takahashi and A. L. Fink, *Biochemistry*, 29 (1990) 3480.
26. S.Chakraborty and C. R. Raj, *J. Electroanal. Chem.*, 609 (2007) 155.
27. R. Geng, G. Zhao, M. Liu and M. Li, *Biomaterials*, 29 (2008) 2794.
28. X. Han, W. Huang, J. Jia, S. Dong and E. Wang, *Biosens. Bioelectron.*, 17 (2002) 741.
29. J. S. Xu, G. C. Zhao, *Int. J. Electrochem. Sci.*, 3 (2008) 519.
30. A.J. Bard and L. R. Faulkner, *Electrochemical Methods Fundamentals and Applications*, John Wiley & Sons, Inc, (2001)